Mechanical and Thermal Properties of Biocomposites from Poly(lactic acid) and DDGS

Yonghui Li, Xiuzhi Susan Sun

Department of Grain Science and Industry, Bio-Materials and Technology Lab, Kansas State University, Manhattan, Kansas 66506

Received 27 May 2010; accepted 31 October 2010
DOI 10.1002/app.33681
Published online 22 February 2011 in Wiley Online Library (wileyonlinelibrary.com).

ABSTRACT: Distillers dried grains with solubles (DDGS), an ethanol industry coproduct, is used mainly as a low-value feedstuff. Poly(lactic acid) (PLA) is a leading biodegradable polymer, but its applications are limited by its relatively high cost. In this study, low-cost, high-performance biodegradable composites were prepared through thermal compounding of DDGS and PLA with methylene diphenyl diisocyanate (MDI) as a coupling agent. Mechanical, morphological, and thermal properties of the composites were studied. The coupling mechanism of MDI in the PLA/DDGS system was confirmed via Fourier-transform infrared spectra. The PLA/20% DDGS composite with 1% MDI showed tensile strength (77 MPa) similar to that of pure PLA, but its Young's modulus was 25% higher than that of pure PLA. With MDI, strong interfacial adhesion was established between the PLA matrix and DDGS particles, and the porosity of the composites decreased dramatically. Crystallinity of PLA in the composites was higher than that in pure PLA. Composites with MDI had higher storage moduli at room temperature than pure PLA. This novel application of DDGS for biocomposites has significantly higher economic value than its traditional use as a feedstuff. © 2011 Wiley Periodicals, Inc. J Appl Polym Sci 121: 589–597, 2011

Key words: poly(lactic acid) (PLA); distillers dried grains with solubles (DDGS); biodegradable composites; thermomechanical properties

INTRODUCTION

The U.S. ethanol industry has grown exponentially in recent years, and the supply of distillers dried grains with solubles (DDGS) has subsequently increased dramatically. In 2006, about 13.2 million metric tons of DDGS were produced in the United States, and this number may increase to 25 million metric tons by 2011.[1] DDGS contains about 26.8–33.7% protein (dry weight basis), 39.2–61.9% carbohydrates (including fibers), 3.5–12.8% oils, and 2.0–9.8% ash.[2] Currently, the ethanol industry's only outlet for DDGS is animal feed ingredients.[3,4] Most research publications about DDGS focus on its feed applications.[5–7]

In recent years, DDGS production has far exceeded its consumption rate as feed. It is predicted that DDGS may have to be disposed of via landfilling, creating an environmental burden.[3] Consequently, development of new outlets for DDGS has become an urgent need and is crucial to maintaining economic viability of the ethanol industry. Several potential alternatives have been proposed including extracting higher value protein and cellulose from DDGS[8,9] and using DDGS for phenolic/DDGS composites,[10,11] biocomposites,[3,12] and bioadhesives.[13] In this study, we explore the feasibility of using DDGS for biodegradable composites with poly(lactic acid) (PLA).

PLA is derived from sugar-based materials. It is the leading biodegradable polymer and considered a sustainable alternative to petroleum-based plastics. PLA exhibits mechanical properties similar to those of some traditional polymers. However, its applications are limited by several unsatisfactory characteristics, such as modest strength and modulus, brittleness, low heat distortion temperature, and relatively high cost (~ 80 cents per pound). Therefore, PLA has been compounded with various low-cost natural biopolymers including wood flour, sugar cane, lignin, flax, soy flour, soy protein, and starch to reduce its cost and enhance its modulus and biodegradability.[14–23] Our group has made achievements in preparing PLA/starch composites. When a mixture of 55% PLA and 45% starch (w/w) was thermally compounded with 0.5% methylene diphenyl diisocyanate (MDI) as coupling agent, the composite showed enhanced mechanical properties and storage modulus above glass transition temperature.[24,25]

DDGS is a multiple-component biopolymer that has not been studied for use in PLA composites but

Correspondence to: X. Susan Sun (xss@ksu.edu).
This article is Kansas Agricultural Experiment Station contribution 10-315-J

Journal of Applied Polymer Science, Vol. 121, 589–597 (2011)

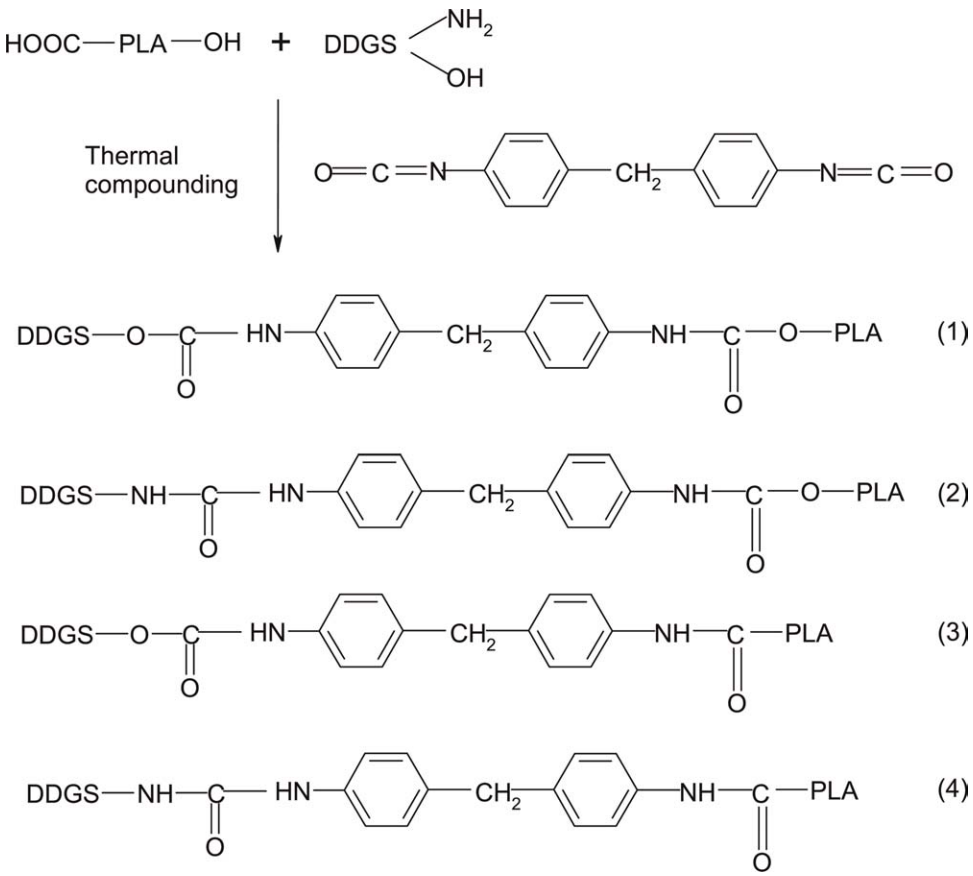

Figure 1 Proposed coupling mechanism between PLA and DDGS with MDI.

exhibits several advantages over other fillers. First, the cost of DDGS is only 4–6 cents per pound, which is lower than the cost of starch (10–20 cents per pound), wood fibers (~ 10 cents per pound), and soy flour (~ 10 cents per pound). Second, DDGS contains about 30% zein, which is a hydrophobic protein and has been considered a candidate for adhesives.[26] For that reason, zein might provide extra hydrophobic interactions and adhesion with the PLA matrix in PLA/DDGS composites. MDI used as a coupling agent for the PLA/DDGS system could further improve compatibility and interfacial adhesion. MDI has two isocyanate groups, which react with nucleophiles such as hydroxyl groups, carboxyl groups, and amino groups to form urethane or urea linkages.[18,23,27] Consequently, MDI can act as a chain extender for pure PLA, which has been reported in detail by Chen et al.[18] However, no significant effect of MDI on the thermal and mechanical properties of pure PLA were observed.[18] Therefore, the coupling reaction of pure PLA with MDI was not included in this study. The proposed coupling mechanism between PLA and DDGS with MDI is shown in Figure 1. Potential applications for these novel composites include vehicle interiors, appliance components, service utensils, and packaging materials. The objectives of this study were to develop value-added biocomposites from DDGS with PLA matrix and investigate the composites' mechanical, morphological, and thermal properties.

EXPERIMENTAL

Materials

PLA (2002D) in pellet form was obtained from NatureWorks LLC (Minnetonka, MN). Corn DDGS was provided by Abengoa Bioenergy (York, NE) and contained 57% carbohydrates, 31% crude protein, and 9% crude fat based on dry matter. MDI was purchased from ICI Polyurethanes Group (West Deptford, NJ).

Preparation of PLA/DDGS composites

PLA pellets were ground through a 2-mm screen in a laboratory mill (Thomas-Wiley, Philadelphia, PA). DDGS was also ground with the same mill through a 1-mm screen. Ground PLA and DDGS were dried in a vacuum oven at 80°C for 24 h. Mixtures of ground PLA with 20, 30, 40, or 50% DDGS (based on total weight) were mixed in a stand mixer (Ultra

Power Kitchen Aid, St. Joseph, MI) for 10 min and then transferred to an intensive mixer (Rheomix 600, Haake, Paramus, NJ) equipped with two corotating rollers with a gap. The mixtures were thermal blended for 3 min at 180°C and 130 rpm. When cool, mixtures were ground into 2 mm powder. Pure PLA was treated with the same procedures as the control. Composites of PLA/20% DDGS with varying ratios of MDI (0.25, 0.5, 1, and 2% based on 100 parts of PLA/DDGS mixture) were prepared similarly to further investigate the effectivity of MDI as coupling agent. Dog-bone-type tensile bars were compression molded at 180°C and 8000 lb for 5 min with a Carver hot press (model 3889, Auto "M," Carver, Wabash, IN) according to ASTM Method D 638-91,[28] cooled to room temperature in air, and then removed from the mold. Five tensile bars were prepared for each type of composite, and bars were conditioned at 25°C with a relative humidity of 50% for at least 48 h prior to characterization.

Fourier-transform infrared spectroscopy

Fourier-transform infrared (FTIR) spectra of the samples were acquired with a Perkin–Elmer Spotlight 300 spectrometer. Spectra were collected in the region of 4000 to 800 cm^{-1} with a spectral resolution of 8 cm^{-1} and 64 scans coadded. At least three replicates were collected for each sample type.

Mechanical measurements

The tensile tests were performed with an Instron testing system (model 4465, Canton, MA) at a crosshead speed of 5 mm/min with a 30 mm gauge length. Five replicates were tested for each sample type.

Scanning electron microscopy

Morphology of the fractured surfaces of composites obtained from tensile tests was observed via scanning electron microscopy (SEM; Hitachi *S*-3500*N*, Hitachi Science Systems, Japan). Each specimen was mounted on an aluminum stub, and the fractured surface was coated with an alloy of 60% gold and 40% palladium with a sputter coater (Desk II Sputter/Etch Unit, NJ) before observation. DDGS was observed similarly.

Differential scanning calorimetry

Thermal transitions of the composites were measured with a TA differential scanning calorimetry (DSC) Q200 instrument in an inert environment by using nitrogen with gas flow rate of 50 mL/min. About 5 mg of each sample obtained from a tensile bar was crimp sealed in an aluminum pan. An empty pan was used as a reference. The sample was heated from 0 to 190°C at a rate of 10°C/min to examine the glass transition temperature (T_g) and crystallinity of PLA in the test specimens. Crystallinity (X_m) was estimated according to the following equation:

$$X_m(\%) = \frac{\Delta H_m}{\Delta H_0 \times X_{\mathrm{PLA}}} \times 100 \quad (1)$$

ΔH_m and ΔH_0 are heats (J/g) of melting of composite and PLA crystal of infinite size with a value of 93.6 J/g,[29] respectively, and X_{PLA} is the PLA fraction in the composite.

Thermogravimetric analysis

Thermal stability of the samples was determined with a Perkin–Elmer Pyris1 thermogravimetric analysis (TGA) instrument (Norwalk, CT). About 5 mg of each sample obtained from a tensile bar was placed in the pan and heated from 40 to 600°C at a heating rate of 20°C/min under a nitrogen atmosphere.

Dynamic mechanical analysis

Dynamic mechanical experiments were conducted using a Perkin–Elmer dynamic mechanical analysis (DMA) 7e instrument (Norwalk, CT) in a three-point flexural mode at 1 Hz frequency. Specimens (about $10 \times 6 \times 2$ mm^3) were obtained from tensile bars with a saw, and the edges were polished carefully with grade 240 abrasive sandpaper. Specimens were heated from 0 to 150°C at a heating rate of 3°C/min under a helium atmosphere. Flexural storage modulus and flexural loss modulus were determined from the changes in the amplitude and phase angle of the observed oscillating strain within the approximation of linear response of the specimen.

RESULTS AND DISCUSSION

Fourier-transform infrared spectra

Figure 2 shows the representative FTIR spectra of MDI, DDGS, PLA, and the PLA/20% DDGS/1% MDI composite. The strong absorption peak at 2292 cm^{-1} for MDI was attributed to the free —N=C=O groups. For DDGS, the broad band centered at 3364 cm^{-1} was assigned to the stretching vibration of —OH and —NH from carbohydrates and protein, the peak at 2930 cm^{-1} to the stretching of —CH from lipids, the peak at 1654 cm^{-1} to the amideI absorption of corn protein, and the peaks at the region of 1250–1000 cm^{-1} to carbohydrates. These results

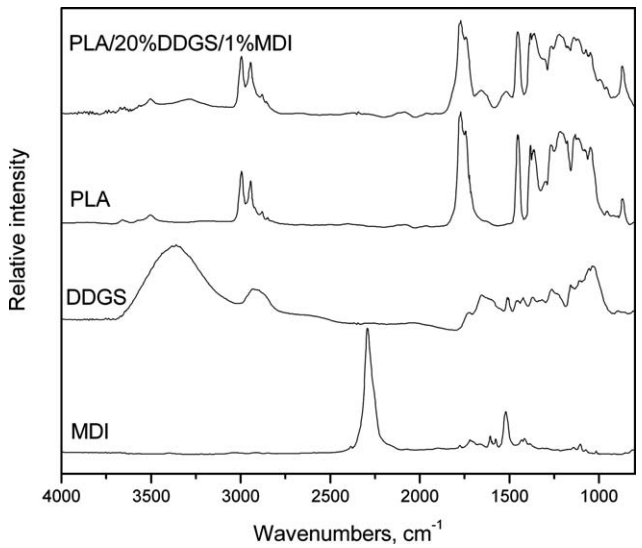

Figure 2 FTIR spectra of MDI, DDGS, PLA, and PLA/20% DDGS/1% MDI composite.

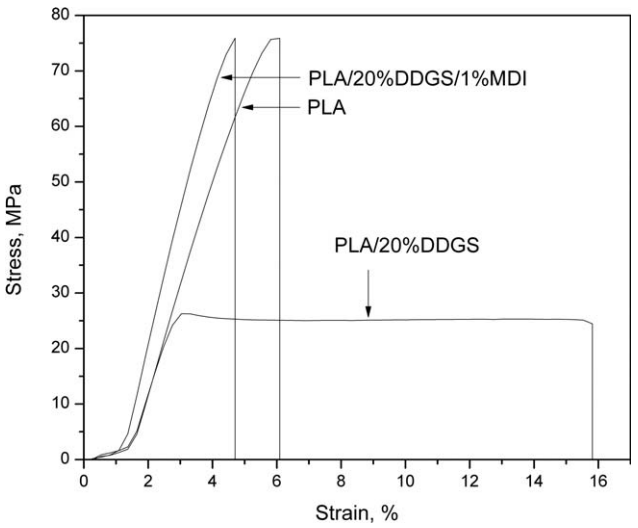

Figure 3 Tensile stress–strain curves of PLA and typical PLA/DDGS composites.

confirm that DDGS is composed of carbohydrates, protein, and lipids. PLA exhibited —OH vibration bands at 3500 cm^{-1}; —CH stretching and bending vibration bands at 2994, 2944, and 1454 cm^{-1}; and —C=O vibration bands at 1772 cm^{-1}.[30] After thermal compounding of PLA and DDGS with MDI, the peak of —N=C=O in the composites totally disappeared, indicating that all free isocyanate groups from MDI were consumed during thermal compounding. Moreover, the strong absorption peak of —OH and —NH observed in DDGS became very weak, indicating that most —OH and —NH groups were reacted with MDI in forming urethane and urea linkages. The urea–urethane and alcohol–urethane groups were expected to be found at 1647 cm^{-1} and 1704–1727 cm^{-1},[3] respectively, which were overlapped with amideI and —C=O absorption.

Mechanical properties

Pure PLA exhibited tensile strength (σ) of 77 MPa, elongation (ε) of 6.2%, and Young's modulus (*E*) of 2.0 GPa (Table I). With 20% DDGS, σ and *E* decreased to 27 MPa and 1.8 GPa, respectively, whereas ε increased significantly to 16%, as shown in the stress–strain curve (Fig. 3). As the DDGS loading further increased, σ and *E* kept decreasing, whereas ε remained higher than that of pure PLA. When DDGS content reached 50% in the composite, σ and *E* decreased to about 10 MPa and 0.8 GPa, respectively, and ε was 7.8% (Table I). These results indicated that interfacial adhesion between the PLA matrix and DDGS particles was poor because of their immiscible characteristics. The loading ratio of DDGS was then fixed at 20% to investigate the effect of coupling agent (MDI) on mechanical properties of composites (Table II). The σ and *E* of PLA/20% DDGS composites increased dramatically by incorporating MDI, compared with composites without MDI, whereas ε decreased slightly compared with that of pure PLA. With 0.25% MDI, σ and *E* increased to 54 MPa and 2.4 GPa, respectively. For composites with 0.5% MDI, σ further increased to 68 MPa, whereas *E* remained almost unchanged. Optimum mechanical properties were obtained at 1% MDI, at which σ (77 MPa) was the same as that of pure PLA, *E* (2.5 GPa) was 25% higher, and ε (5.0%) was slightly decreased. As MDI ratio further increased to 2%, mechanical properties decreased.

TABLE I
Mechanical Properties of PLA/DDGS Composites Without Coupling Agent

Sample	Tensile strength (MPa)	Elongation at break (%)	Young's modulus (MPa)
Pure PLA	77.10 ± 0.76	6.18 ± 0.37	2.04 ± 0.02
20% DDGS	27.44 ± 0.68	15.65 ± 2.36	1.81 ± 0.04
30% DDGS	20.24 ± 1.11	11.62 ± 2.08	1.51 ± 0.05
40% DDGS	13.55 ± 0.94	10.95 ± 3.57	1.20 ± 0.14
50% DDGS	9.72 ± 0.51	7.77 ± 1.90	0.80 ± 0.05

TABLE II
Mechanical Properties of PLA/20% DDGS Composites with Varying Amount of MDI as Coupling Agent

Sample	Tensile strength (MPa)	Elongation at break (%)	Young's modulus (MPa)
0.25% MDI	54.47 ± 1.34	3.92 ± 0.12	2.36 ± 0.09
0.5% MDI	68.13 ± 0.79	4.56 ± 0.16	2.41 ± 0.05
1% MDI	77.05 ± 1.70	4.96 ± 0.16	2.52 ± 1.26
2% MDI	68.77 ± 0.45	4.84 ± 0.36	2.36 ± 0.04

As expected, DDGS particles in the PLA matrix without a coupling agent acted as stress concentrators under tensile stress, often inducing fractures and resulting in low tensile strength. Moreover, because of the poor packing properties of DDGS, some pores were observed in the tensile bars without MDI, which also resulted in low strength. However, in contrast to the immediate fracture after reaching maximum load for PLA, the PLA/20% DDGS composite showed distinct yielding and stable neck growth (Fig. 3), which were induced by the debonding of DDGS particles from the PLA matrix during fracturing. This is further discussed in the morphology section.

Because of the formation of covalent linkages between hydroxyl or carboxyl groups from PLA into PLA–MDI and hydroxyl or amine groups from DDGS into DDGS–MDI (Fig. 1), interfacial adhesion between the PLA matrix and DDGS particles was greatly improved, resulting in increased strength and modulus. Meanwhile, with formation of DDGS–MDI, packing properties of DDGS were improved, and porosity of the composites significantly decreased as indicated in the SEM images (Fig. 4), which also enhanced mechanical properties. However, excess PLA–MDI and DDGS–MDI segments were formed with extra MDI (2%), and these segments might interfere with effective entanglements or segmental crystallization between DDGS particles and the PLA matrix,[31] resulting in decreased strength and modulus. Similar results were reported for PLA/sugar beet pulp composites with MDI ranging from 0 to 3%.[18]

Morphology

As shown in Figure 4, DDGS exists in irregular shapes and various sizes (20–200 μm) and has coarse surfaces. Pure PLA has a smooth and continuous fracture surface, indicating a brittle fracture behavior that corresponds to its low elongation value shown in Table I. Surface roughness of the PLA matrix obviously increased with inclusion of 20% DDGS as observed from SEM images [Fig. 4(a,a′)], indicating that remarkable plastic deformation occurred. As discussed previously, because there was not sufficient interfacial adhesion, DDGS particles debonded from the PLA matrix at the interface during fracturing. Void formation due to cavitation localized at the particle/matrix interfaces was visible together with PLA matrix strands surrounding voids [Fig. 4(a,a′)], and the stress state in the PLA matrix was altered. During the debonding process, these PLA matrix strands were plastically stretched, fibrillized, and finally broken down. The toughening mechanism of particle-filled semicrystalline polymers has been explained in detail.[32,33] With the naked eye and SEM, we also observed some pores attributed to the poor packing properties of DDGS. As DDGS loading ratio further increased, more pores were observed (SEM images not shown), which corresponds to the decreased strength and elongation of composites.

With 0.25% MDI added, fracturing extending through DDGS particles was observed in addition to debonding, and the porosity decreased obviously [Fig. 4(b)], indicating the greatly improved wettability of DDGS particles by the PLA matrix and penetration of PLA into the porous DDGS. With increasing amounts of MDI, almost no evidence of debonding could be observed at the fracture surfaces [Fig. 4(c–e)]. Instead, DDGS particles ruptured together with the PLA matrix at the plane of the fracturing surfaces. For composites with 1 and 2% MDI, few individual DDGS particles could be observed, and those that were distinguishable appeared to be completely coated and penetrated by the PLA matrix [Fig. 4(d–e)]. Moreover, no pores could be observed in the tensile bars. The SEM images provide clear evidence that MDI addition established strong interfacial bonding between the PLA matrix and DDGS particles that led to greatly improved stress transfer between the matrix and fillers, corresponding to measurements of the mechanical properties.

Thermal properties

Figure 5 shows DSC thermograms of compression-molded PLA and PLA/20% DDGS composites. The thermograms were obtained from the first heating scan to reveal the glass transition and crystalline status of the PLA component in the composites. Table III summarizes the DSC results. The T_g of the composite without MDI was 3°C lower than that of pure PLA (62.1°C). With addition of MDI, T_g increased slightly, indicating that some coupling effects from MDI occurred. An endothermic peak around the glass transition region was observed for PLA and composites because of physical aging during storage at ambient temperature. The peak area of PLA, PLA composites without MDI and with 0.25% MDI was larger than that of composites with a higher MDI loading ratio. During sample storage, molecular mobility reduces free volume. Samples with a higher degree of aging have smaller free volume as well as smaller enthalpy and potential energy than samples with a lower degree of aging.[34] Therefore, when the aged samples are heated, more energy is required for the glass transition, thus increasing the area of the endothermic peak. Crystallinity of PLA in the composites was higher than that of pure PLA. However, crystallinity of the composite with 2% MDI was slightly lower than that of other composites. This might be caused by the excess PLA–MDI and DDGS–MDI segments that occurred

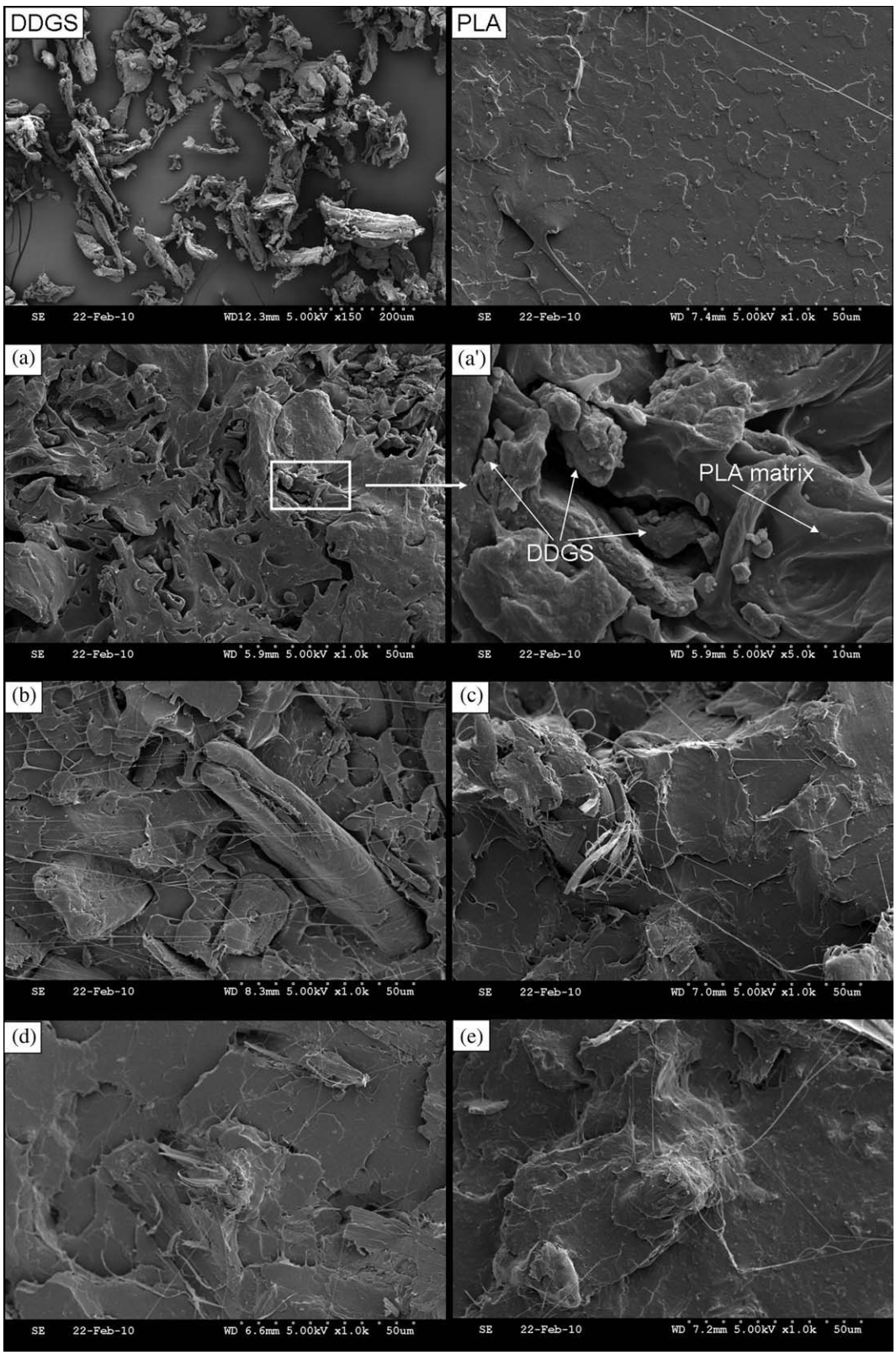

Figure 4 SEM images of PLA and PLA/20% DDGS composites with (a and a′) 0% MDI, (b) 0.25% MDI, (c) 0.5% MDI, (d) 1% MDI, and (e) 2% MDI.

with extra MDI loading, which would interfere with segmental crystallization, as discussed previously in the mechanical properties section.

TGA and derivative TGA thermograms of DDGS, PLA, and PLA/20% DDGS composites are shown in Figure 6(A,B), and the TGA data are summarized in

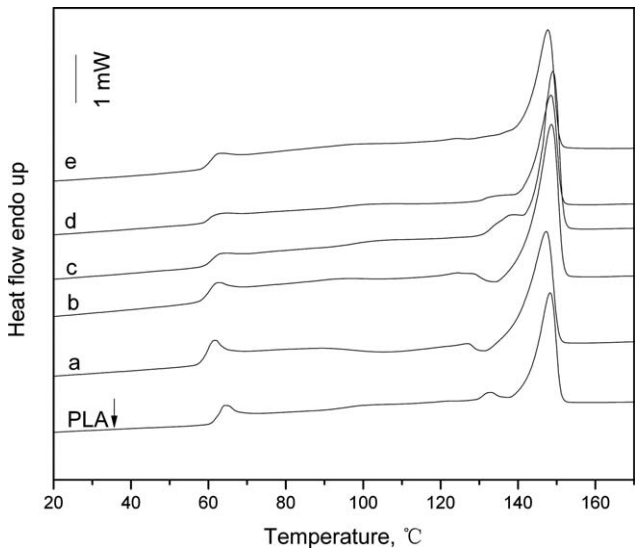

Figure 5 DSC thermograms of PLA and PLA/20% DDGS composites with (a) 0% MDI, (b) 0.25% MDI, (c) 0.5% MDI, (d) 1% MDI, and (e) 2% MDI (first scan).

Table IV. Because of its multiple components (carbohydrates, protein, lipids, etc.), DDGS exhibited a much broader decomposition range than PLA; onset, end, and peak decomposition temperatures (T_{onset}, T_{end}, and T_{max}) of DDGS were 298.8, 418.6, and 383.1°C, respectively, and T_{onset}, T_{end}, and T_{max} of PLA were 344.5, 388.9, and 381.7°C, respectively. The composite without MDI showed slightly higher decomposition temperatures than PLA with T_{end} and T_{max} of 401.2 and 385.5°C, respectively. All composites with MDI showed similar decomposition temperatures with T_{max} values slightly lower than that of PLA. Because DDGS has higher tar and ash content than PLA, the residue weight of PLA/DDGS composites above 425°C is higher than that of PLA but lower than that of DDGS.

For PLA and PLA/20% DDGS composites with and without MDI, storage modulus (E') increased gradually with heating between 20 and 61°C, reached a peak value, dropped sharply at the glass transition region, and then reached a rubbery plateau [Fig. 7(A)]. The increase of E' between 20 and 61°C was a kinetic unfreezing of a nonequilibrium disordered structure at the low heating rate (3°C/min) and sinusoidal frequency (1 Hz) and a consequence of molecular structure densification and aging.[23] For all samples, the competing effects of

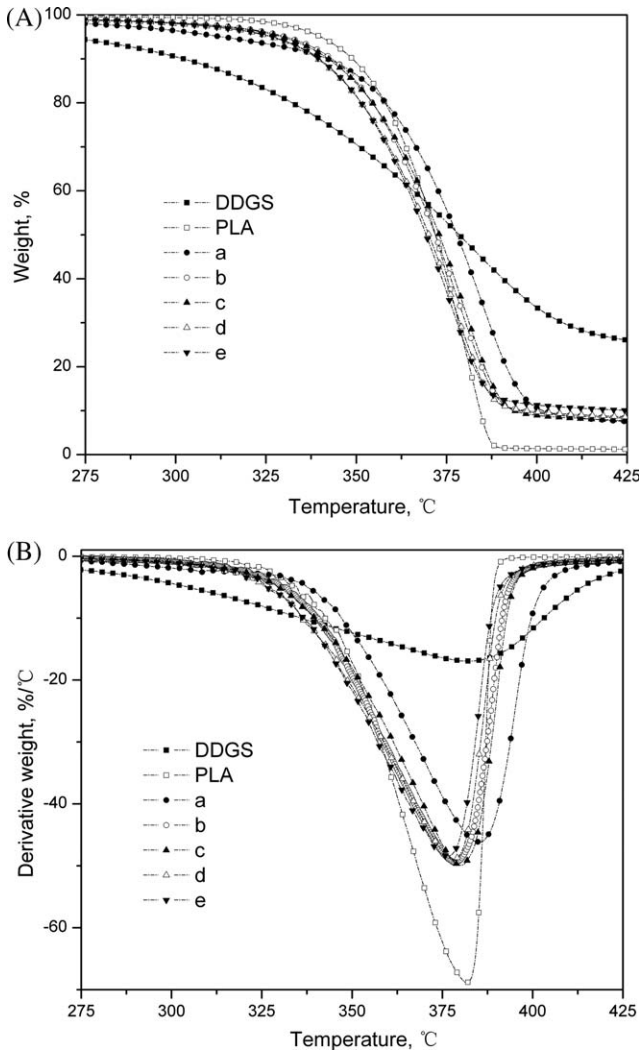

Figure 6 TGA (A) and derivative TGA (B) thermograms of DDGS, PLA, and PLA/20% DDGS composites with (a) 0% MDI, (b) 0.25% MDI, (c) 0.5% MDI, (d) 1% MDI, and (e) 2% MDI.

TABLE III
DSC Results of PLA and PLA/20% DDGS Composites with Varying Amount of MDI

Sample	T_g (°C)	ΔC_p (J/g)·(°C)	T_m (°C)	ΔH_m (J/g)	X_m (%)
PLA	62.1	0.35	148.3	19.01	20.3
0%MDI	58.9	0.38	147.3	19.94	26.6
0.25%MDI	59.7	0.30	148.6	19.69	26.3
0.5%MDI	60.8	0.27	148.9	19.66	26.3
1%MDI	60.3	0.26	148.5	18.72	25.0
2%MDI	60.5	0.35	147.7	16.96	22.7

TABLE IV
Decomposition Temperatures of DDGS, PLA, and PLA/20% DDGS Composites with Varying Amount of MDI Determined from Derivative TGA Thermograms

Sample	T_{onset} (°C)	T_{end} (°C)	T_{max} (°C)
DDGS	298.8	418.6	383.1
PLA	344.5	388.9	381.7
0% MDI	343.0	401.2	385.5
0.25% MDI	340.2	394.2	379.9
0.5% MDI	341.7	393.2	378.4
1% MDI	335.5	391.2	377.8
2% MDI	337.2	389.7	376.5

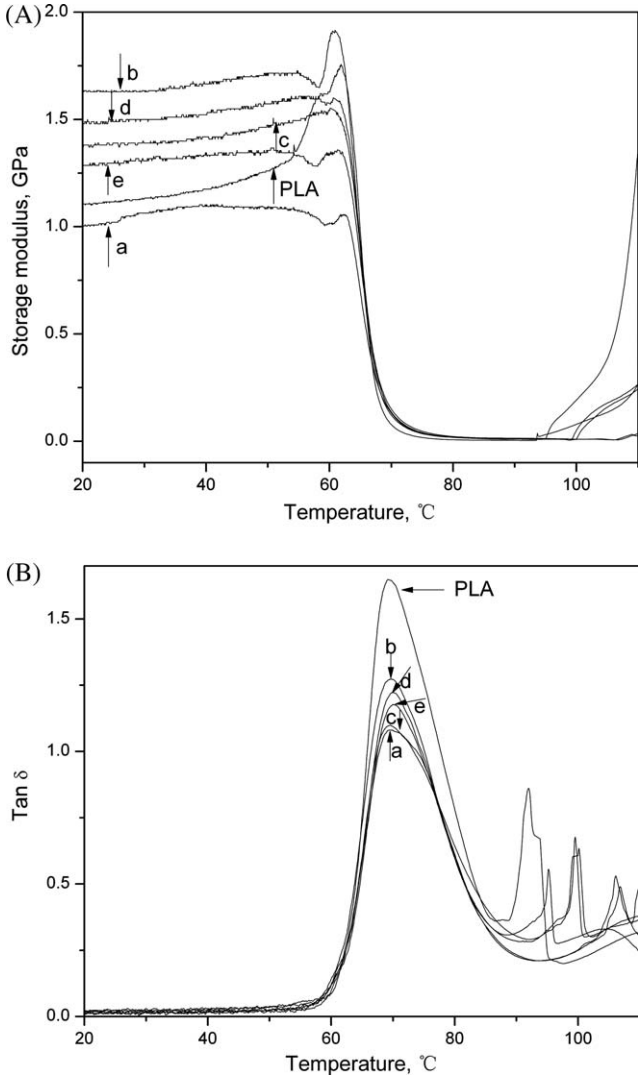

Figure 7 Flexural storage modulus (A) and tan δ (B) of PLA and PLA/20% DDGS composites with (a) 0% MDI, (b) 0.25% MDI, (c) 0.5% MDI, (d) 1% MDI, and (e) 2% MDI.

aging and relaxation led to the fluctuation of E' before its sharp drop. An increase in E' around 100°C was attributed to cold crystallization of PLA components. When the E' values of PLA and composites at room temperature (25°C) were compared, composites without MDI showed a smaller E' (1.02 GPa) than PLA (1.12 GPa), corresponding to its lower mechanical strength. With MDI, an obvious increase in E' was observed for all composites, indicating effective coupling between PLA and DDGS.

The loss factor (tan δ) of PLA and PLA/20% DDGS composites during heating is presented in Figure 7(B). The peak that appeared at about 69°C is known as T_g from DMA measurement. Pure PLA had the largest tan δ (1.65) at T_g, indicating that it contains a greater amorphous phase portion than the composites, which corresponds to the lowest crystallinity value of pure PLA determined from DSC. In a composite system with filler, the filler would limit mobility of the matrix molecular chain, thereby affecting relaxation of the matrix chains and causing a lower damping in the transition zone compared with a pristine polymer.[35]

CONCLUSION

PLA/DDGS composites with mechanical properties similar to those of pure PLA were successfully prepared via thermal compounding. FTIR spectroscopy verified that MDI was an effective coupling agent for the PLA/DDGS system. Without a coupling agent, tensile strength and Young's modulus of composites decreased dramatically as DDGS content increased. For PLA/20% DDGS composites, as MDI loading ratio gradually increased from 0.25 to 1%, tensile strength and Young's modulus increased and approached values similar to those of pure PLA. Morphology of the fracture surfaces showed that addition of MDI established strong interfacial bonding between the PLA matrix and DDGS particles and decreased the porosity of composites. Crystallinity of PLA in the composites was higher than that of pure PLA. Composites with MDI had higher storage moduli at room temperature than pure PLA. These results indicate that using low-cost DDGS as filler can result in biodegradable composites that have properties similar to those of pure PLA but cost significantly less. This novel application of DDGS for biocomposites has significantly higher economic value than its traditional use as a feedstuff.

References

1. Robinson, P. H.; Karges, K.; Gibson, M. L. Anim Feed Sci Tech 2008, 146, 345.
2. Rosentrater, K. A.; Muthukumarappan, K. Int Sugar J 2006, 108, 648.
3. Wu, Q.; Mohanty, A. K. J Biobased Mater Bioenergy 2007, 1, 257.
4. Cheesbrough, V.; Rosentrater, K. A.; Visser, J. J Polym Environ 2008, 16, 40.
5. Chevanan, N.; Rosentrater, K. A.; Muthukumarappan, K. Cereal Chem 2008, 85, 132.
6. Li, M. H.; Robinson, E. H.; Oberle, D. F.; Lucas, P. M. Aquacult Nutr 2010, 16, 188.
7. Xu, G.; Baidoo, S. K.; Johnston, L. J.; Bibus, D.; Cannon, J. E.; Shurson, G. C. J Anim Sci 2010, 88, 1388.
8. Xu, W.; Reddy, N.; Yang, Y. Carbohydr Polym 2009, 76, 521.
9. Wang, Y.; Tilley, M.; Bean, S.; Sun, X. S.; Wang, D. J Agr Food Chem 2009, 57, 8366.
10. Tatara, R. A.; Rosentrater, K. A.; Suraparaju, S. Ind Crop Prod 2009, 29, 9.
11. Tatara, R. A.; Suraparaju, S.; Rosentrater, K. A. J Polym Environ 2007, 15, 89.
12. Schilling, C. H.; Karpovich, D. S.; Tomasik, P. J Biobased Mater Bioenergy 2009, 3, 408.
13. Mohanty, A. K.; Wu, Q.; Singh, A. U. S. Pat. 20070196521, A1, 2007.

14. Ke, T. Y.; Sun, X. S. Cereal Chem 2000, 77, 761.
15. Li, J C.; He, Y.; Inoue, Y. Polym Int 2003, 52, 949.
16. Zhang, J. F.; Sun, X. S. Biomacromolecules 2004, 5, 1446.
17. Zhang, J. W.; Jiang, L.; Zhu, L. Y. Biomacromolecules 2006, 7, 1551.
18. Chen, F.; Liu, L.; Cooke, P. H.; Hicks, K. B.; Zhang, J. Ind Eng Chem Res 2008, 47, 8667.
19. Wang, N.; Yu, J. G.; Chang, P. R.; Ma, X. F. Carbohydr Polym 2008, 71, 109.
20. Duhovic, M.; Horbach, S.; Bhattacharyya, D. J Biobased Mater Bioenergy 2009, 3, 188.
21. Fang, K.; Wang, B. B.; Sheng, K. C.; Sun, X. S. J Appl Polym Sci 2009, 114, 754.
22. Ren, J.; Fu, H. Y.; Ren, T. B.; Yuan, W. Z. Carbohydr Polym 2009, 77, 576.
23. Li, Y.; Venkateshan, K.; Sun, X. S. Polym Int 2010, 59, 1099.
24. Wang, H.; Sun, X. S.; Seib, P. J Appl Polym Sci 2001, 82, 1761.
25. Wang, H.; Sun, X. S.; Seib, P. J Appl Polym Sci 2002, 84, 1257.
26. Parris, N.; Dickey, L. C. J Agr Food Chem 2003, 51, 3892.
27. Dieteroch, D.; Grigat, E.; Hahn, W. In Polyurethane Handbook; Oertel, G., Ed.; Hanser: New York, 1985; p 7.
28. ASTM D 638-91. In Annu Book of ASTM Standards; American Society for Testing and Materials: Philadelphia, 1992; Vol. 8.01, p 161.
29. Fischer, E. W.; Sterzel, H. J.; Wegner, G. Kolloid-Z Z Polym 1973, 251, 980.
30. Li, Y.; Sun, X. S. Biomacromolecules 2010, 11, 1847.
31. Zhang, C.; Li, K.; Simonsen, J. Polym Eng Sci 2006, 46, 108.
32. Kim, G. M.; Michler, G. H. Polymer 1998, 39, 5689.
33. Kim, G. M.; Michler, G. H. Polymer 1998, 39, 5699.
34. Pan, P.; Zhu, B.; Inoue, Y. Macromolecules 2007, 40, 9664.
35. Nielsen, L. E.; Landel, R. F. Mechanical Properties of Polymers and Composites, 2nd ed; Marcel Dekker: New York, 1994; p 425.